The Inhibitory Effects of Hypericin Nano-spheres on the Proliferation of HepG2 Cells and HeLa Cells

Hong XUE[1#], Chunmei LI[1#], Hongyan WU[1], Jie LAN[1], Jialong LU[1], Yiting YANG[1], Yujie XU[1], Yihe WEI[1], Zhiqiang CHEN[2*], Xin JIANG[2*], Dengfeng ZOU[1,3*]

1. College of Pharmacy, Guilin Medical University, Guilin 541199, China; 2. Guangxi Clinical Medical Research Center for Neurological Diseases, First Affiliated Hospital of Guilin Medical University, Guilin 541001, China; 3. Key Laboratory of Early Prevention and Treatment of Regional High Frequency Tumors, Ministry of Education, Guangxi Medical University; Key Laboratory of Early Prevention and Treatment of Regional High Frequency Tumors in Guangxi, Nanning 530021, China

Abstract To explore the distinct effects of hypericin nanoparticles (HC-NPs) on tumor cell growth, water-soluble HC-NPs were prepared from hypericin and its aqueous solution (HC) and used to treat HepG2 hepatocellular carcinoma cells and HeLa uterine cervical cancer cells. The cell viability of HepG2 and HeLa cells was assessed using the CCK-8 assay, and the IC_{50} values were determined. The cell migration was evaluated using a scratch wound healing assay to compare the effects of HC-NPs and HC. Experimental findings revealed that both HC and HC-NPs exerted suppressive effects on the vitality of HepG2 and HeLa cells, as indicated by the CCK-8 assay. The IC_{50} values for HC against tumor cells were identified as 71.00 and 124.35 μg/ml, respectively, while for HC-NPs, these were 27.48 μg/ml for HepG2 cells and 61.00 μg/ml for HeLa cells. The scratch assay demonstrated that HC and HC-NPs effectively hindered cell migration and diminished the rate of wound closure. The live/dead cell co-staining assay further confirmed the suppressive effects of HC and HC-NPs on cell proliferation, with the nanoformulation exhibiting a more pronounced effect. The data suggest that HC-NPs are considerably more effective at inhibiting the proliferation of HepG2 and HeLa cancer cells compared to HC. Subsequently, the binding site of the drug on the cells was identified using laser confocal microscopy. Additionally, flow cytometry and laser confocal microscopy were employed to investigate the generation of reactive oxygen species. In conclusion, the findings of this study highlight the potent inhibitory effects of HC-NPs on the growth of HepG2 and HeLa cancer cells, underscoring their potential as therapeutic agents in cancer treatment.

Key words Human cancer cells; Hypericin; Nanoparticles; Proliferative inhibition; Cytotoxicity

DOI: 10.19759/j.cnki.2164-4993.2026.02.001

Liver cancer, a significant health challenge globally, particularly in regions with high prevalence of viral hepatitis, poses a substantial threat to human health. It often arises against a backdrop of cirrhosis and inflammation, with advanced cases leading to a generally poor prognosis for affected individuals[1]. In China, primary liver cancer stands as one of the leading cancers, with a notable mortality rate that ranks it second among cancer-related deaths. The incidence of liver cancer is not only high, but also shows a concerning trend of young cells, affecting individuals at a younger age than previously observed[2].

The complexity of primary liver cancer is further underscored by its heterogeneity and the variability in treatment options across different regions. These regional differences are influenced by factors such as the availability of healthcare resources and the prevalence of specific risk factors, such as viral hepatitis. The standard approach to managing this diverse malignant tumor often involves multimodal therapy tailored to the specific needs and circumstances of each patient[3]. However, the effectiveness of these treatments can vary, and there is a continuous search for more effective and less toxic therapeutic strategies.

Cervical cancer, another formidable gynecological malignancy, ranks just after breast cancer in terms of incidence among women worldwide. It poses a grave risk to women's health and lives[4]. Conventional treatment methods for cervical cancer, including surgery and chemotherapy[5], while effective in many cases, are not without risks and side effects. Platinum-based chemotherapy, either as monotherapy or in combination with other agents, is a widely used clinical approach[6]. However, for recurrent or metastatic cervical cancer, more specialized treatments such as targeted therapy and immunotherapy have been introduced[7]. Despite these advancements, there are still limitations to the effectiveness of these treatments, and there is an ongoing need for improved therapeutic options.

In light of these challenges, the exploration of novel

Received: December 25, 2025 Accepted: March 7, 2026

Supported by The Project Program of Guangxi Key Laboratory of Drug Discovery and Optimization (GKLPMDDO-2022-C04; GKLPMDDO-2022-C05); 2025 Guangxi Graduate Education Innovation Plan Project (YCSW2025483); College Students Innovation and Entrepreneurship Training Program (YCSW2025483; S202210601139; 202210601037; X202410601225; 202310601038); Key Laboratory of New Processing Technology for Nanferrous Metal & Materials, Ministry of Education/Guangxi Key Laboratory of Optical and Electronic Materials and Devices, Open funds (22KF-22); National Natural Science Foundation of China (32060228); Guangxi Natural Science Foundation Project (2023GXNSFAA026385; 2022JJA140211; 2017GXNSFAA198112; 2019GXNSFAA245077); Research and Innovation Base for Basic and Clinical Application of Nerve Injury and Repair (ZY21195042); Guangxi Key Laboratory of Big Data Intelligent Cloud Management for Neurological Diseases (ZTJ2020005); Guilin Scientific Research and Technology Development Project (20190219 2).

Hong XUE (2001-), female, P. R. China, postgraduate, devoted to research about drug development and conversion.

Chunmei LI (1990-), female, P. R. China, assistant researcher, devoted to research about liver injury.

#These authors contributed equally to this work.

*Corresponding author.

therapeutic agents, such as hypericin nano-spheres, offers a promising avenue for the development of more effective and less toxic cancer treatments. The potential of these nanostructures to inhibit the proliferation of cancer cells, as seen in the case of HepG2 and HeLa cells, could lead to innovative strategies that improve patient outcomes and offer a better quality of life for those battling these diseases. As research progresses, the integration of such novel therapies into clinical practice could mark a significant advancement in the fight against liver and cervical cancers.

The utilization of nano-drug delivery systems (NDDS) represents a significant advancement in the field of targeted cancer therapy. These systems offer a unique approach to enhance the selective delivery of therapeutic agents to cancerous tissues, thereby improving the bioavailability of drugs and minimizing systemic side effects[8]. The application of NDDS involves the strategic modification of drug carriers or the decoration with specific targeting molecules, which allows for more precise drug delivery and increased efficacy.

Hypericin (HC), a naturally occurring anthraquinone compound, has garnered considerable attention due to its potent antitumor properties[9]. It is a natural photosensitizer extracted from the plant *Forsythia suspensa*, commonly referred to as St. John's grass. Research has consistently demonstrated the strong anticancer activity of HC, particularly when used in conjunction with radiation therapy[10]. Despite its high lipid solubility[11], the poor water solubility of HC has been a limiting factor in its clinical application[12]. Addressing this challenge by enhancing the water solubility and bioavailability of HC is a crucial area of focus for research and development.

The advent of nanotechnology has brought forth innovative solutions in the form of nanoparticles, which have emerged as a versatile tool for drug delivery and diagnostics[13]. Cancer cells, characterized by their altered morphology and the formation of new blood vessels, can be targeted by nanoparticles through the recognition of specific biomarkers on the reshaped endothelial cells. This provides a broad array of targets for nanoparticle-based molecular imaging and therapy[14], significantly enhancing the targeting capabilities of cancer treatments.

The application of nanoparticles in drug delivery has been shown to offer a range of benefits. They can improve the water solubility of hydrophobic drugs like HC, increase stability, extend the drug's half-life in the bloodstream[15], and enhance cellular uptake rates[16]. This, in turn, leads to an improved bioavailability of the drug, a reduction in toxicity and side effects[17], and overall, a more effective treatment strategy.

The experimental validation of HC's anti-proliferative effects on HepG2 liver cancer cells and HeLa cervical cancer cells has been demonstrated through various assays, including the CCK-8 assay, scratch assay, and live/dead cell co-staining assay. These studies have consistently shown that HC effectively inhibits the vitality and proliferation of these cancer cells. Laser confocal localization experiments confirmed that hypericin could enter cells and bind to lysosomes. Meanwhile, whether the drug produced reactive oxygen species was detected. The results proved that the drug did not produce reactive oxygen species in HepG2 cells under dark light conditions. Furthermore, the inhibitory effects of HC encapsulated within nanoparticles (HC-NPs) are significantly more potent than those of water-soluble forms of the drug. This enhanced efficacy highlights the potential of HC-NPs as a promising therapeutic strategy for the treatment of liver and cervical cancers, offering a more targeted and less toxic alternative to traditional chemotherapy.

Materials and Methods

Materials

The HepG2 cell line was obtained from the Chinese Academy of Sciences Shanghai Cell Bank. Hypericin was purchased from Lemaitian Pharmaceutical and Desite Biotechnology (batch No. DST220718-024; relative molecular weight: 504.45). It is a brown-black flowable powder with a unique fragrance, a bitter taste, and is insoluble in water. It appears as blue-black or purple-black needle-shaped crystals. Hypericin is readily soluble in pyridine and other organic bases, forming a cherry-red solution with red fluorescence. It is also soluble in aqueous alkaline solutions but almost insoluble in other organic solvents. The solution appears red at pH below 11.5 and green above 11.5, exhibiting red fluorescence. The melting point is >320 ℃.

Reagents

DMEM high sugar (Containing sodium pyruvate) (Beijing Lanjeko Technology Co., Ltd., Beijing, China); 1 × PBS buffer (Beijing Solaibao Technology Co., Ltd., Beijing, China); fetal bovine serum (Ecosa Biotechnology Co., Ltd., Taicang, China); DMSO dimethyl sulfoxide (Beijing Solaibao Technology Co., Ltd., Beijing, China); tetrahydrofuran THF (Xilong Science Co., Ltd., Shantou, China); trypsin EDTA digestive solution (Beijing Solaibao Technology Co., Ltd., Beijing, China); penicillin mixture (100 ×) (Beijing Solebao Technology Co., Ltd., Beijing, China); DSPE-PEG2000 (Xi'an Ruixi Biotechnology Co., Ltd., Xi'an, China); cell counting kit-8 (Dongren Chemical Technology Co., Ltd., Shanghai, China); calcein-AM/PI live/dead cell co-staining experimental detection reagents (Anolun Biotechnology Co., Ltd., Beijing, China); DCFH-DA fluorescent probe reactive oxygen species detection kit (Beyotime Biotech Inc, Shanghai, China); mitochondrial green fluorescent probe (Beyotime Biotech Inc, Shanghai, China); green fluorescent probe for lysosomes (Beyotime Biotech Inc, Shanghai, China).

Experimental equipment

KQ-500E ultrasonic cleaner (Kunshan Ultrasonic Instrument Co., Ltd., Kunshan, China); electric hot air drying oven (Shanghai Boxun Industrial Co., Ltd. Medical Equipment Factory, Shanghai, China); desktop high-speed freezing centrifuge (Thermo Fisher Scientific Co., Ltd., Waltham, Massachusetts, USA); ultrapure water system (Millipore, USA, Milton Burley, Massachusetts); ultra clean workbench (Suzhou Antai Air

Technology Co., Ltd., Suzhou, China); inverted fluorescence microscope (OLYMPUS, Japan, Dongjing, Japan); cell culture incubator (Melt Trading Co., Ltd., Germany, Schwarzbach); enzyme reader (Bole Life Medical Products Co., Ltd., California, USA); ice maker (Panasonic, Japan, Osaka); medical ultra-low temperature refrigerator (Panasonic, Japan, Osaka); laser confocal microscopy (NIS-Elements 5.3, Shanghai, China); flow cytometry (BD, Franklin Hu, New Jersey, USA).

Methods

Preparation of HC-NPs, HC and blank solvents Nano agents and aqueous solvents were prepared using the ultrasonic vibration method, with DESP-PEG2000 as the encapsulation agent, tetrahydrofuran (THF) as the co-solvent, and water as the solvent. A liquid formulation was prepared at a specific ratio and subjected to overnight ultrasonication until successful encapsulation of the drug was achieved. THF was then removed by volatilization at room temperature under sterile conditions. A DESP-PEG2000 blank solvent was prepared using the same procedure. The resulting formulation was stored in the dark at 4 ℃.

Nano particles size detection The morphology of the nanoparticles was determined by transmission electron microscopy (TEM). The solution was shaken with ultrasound for 30 min in advance. A 100 μl pipette was used to aspirate the drug and drop it onto a copper mesh. After the drug was dried in the sun, it was placed under an electron microscope to measure the particle size.

Cell culture HepG2 cells and HeLa cells were resuscitated and both were cultured in 10% fetal bovine serum medium (DMEM : FBS = 9 : 1) at 37 ℃ in a 5% CO_2 incubator.

CCK-8 method for detecting cell proliferation and cytotoxicity Logarithmically growing HepG2 cells and HeLa cells were selected, and a blood cell counting plate was used for cell counting. During seeding, HepG2 cells were seeded on a 96-well plate at a rate of 4×10^3 per well, HeLa cells were seeded under identical conditions. After inoculation, the cells were shaken evenly and laid on a 96-well plate. They were incubated in a cell culture incubator for 24 h and then administered according to the set concentration gradient. Administration was performed in the dark. After 24 h of administration, 10 μl of CCK-8 reagent was added to each well, and the plate was incubated in the incubator for 10 min. The *OD* value was measured using an enzyme-linked immunosorbent assay (ELISA) reader. A blank control group was simultaneously set up to verify whether the solvent produced cytotoxicity.

Cell scratch assay for detecting cell migration Logarithmically growing HepG2 cells and HeLa cells were selected, and a blood cell counting plate was used for cell counting. When seeding the plate, HepG2 cells were seeded at a rate of 1×10^5 per well on a 6-well plate for 3 wells, HeLa cells were seeded at 8×10^4 cells per well under identical conditions. After 24 h of cultivation in a cell culture incubator, the cells grew to 90% – 95%. A 10 μl pipette was used to scratch the surface of the cells. HepG2 cells and HeLa cells were divided into a control group, an NPs IC_{50} group, and an aqueous solvent IC_{50} group, and photos were taken at 0 and 24 h, respectively.

Live/dead cell co staining experiment Logarithmically growing HepG2 cells and HeLa cells were selected, and a blood cell counting plate was used for cell counting. When seeding the plate, HepG2 cells were seeded at a rate of 2×10^4 per well on a 24-well plate for 3 wells, and HeLa cells were seeded under identical conditions. They were incubated in a cell culture incubator for 24 h and then administered according to experimental groups. HepG2 cells and HeLa cells were evenly divided into a control group, an NPs IC_{50} group, and an aqueous solvent IC_{50} group. After administration, the cells were cultured in a cell culture incubator for 24 h, processed, and stained using the Calcein AM/PI assay kit. The concentrations of Calcein AM staining solution and PI staining solution for HepG2 cells were 2.5 and 2.5 μM, respectively; and the concentrations of HeLa cell Calcein AM staining solution and PI staining solution were 2.0 and 1.5 μM, respectively. After processing the cells, cell staining was observed under a laser confocal microscope.

Drug localization experiment Logarithmically growing HepG2 cells and HeLa cells were selected, and a blood cell counting plate was used for cell counting. When seeding the plate, HepG2 cells were seeded at a rate of 2×10^5 per well on a confocal dish for 3 wells, and HeLa cells were seeded at 1×10^5 cells per well under the same conditions. They were incubated in a cell culture incubator for 24 h and then administered according to experimental groups. HepG2 cells and HeLa cells were evenly divided into a control group, an NPs group, and an aqueous solvent group. After administration, the cells were cultured in a cell culture incubator for 24 h. The old medium was discarded, and the cells were rinsed twice with PBS, and then added with the lysosomal probe and incubated in the incubator for 30 min. After removal, the staining solution was discarded and the cells were rinsed twice with PBS, and the anti-fluorescence quencher containing DAPI was added. The concentration of the staining solution was 1 : 2 000. After processing the cells, cell staining was observed under a laser confocal microscope.

Flow cytometry was used to detect the content of ROS after administration Logarithmically growing HepG2 cells and HeLa cells were selected, and a blood cell counting plate was used for cell counting. When seeding the plate, HepG2 cells were seeded at a rate of 6×10^5 per well on a 6-well plate for 3 wells, and HeLa cells were seeded at 4×10^5 cells per well under the same conditions. They were incubated in a cell culture incubator for 24 h and then administered according to experimental groups. HepG2 cells and HeLa cells were evenly divided into a control group, an NPs group, and an aqueous solvent group. After administration, the cells were cultured in a cell culture incubator for 24 h. After treatment, the ROS probe was added, and following 30 min of incubation, the cells were rinsed twice with PBS, and transferred into a flow tube for detection. The concentration of the staining solution was 1 : 4 000.

Confocal laser scanning microscopy was used to detect the content of ROS after administration Logarithmically growing HepG2 cells and HeLa cells were selected, and a blood cell counting plate was used for cell counting. When seeding the plate, HepG2 cells were seeded at a rate of 2×10^5 per well on a confocal dish for 3 wells, and HeLa cells were seeded at 1×10^5 cells per well under the same conditions. They were incubated in a cell culture incubator for 24 h and then administered according to experimental groups. HepG2 cells and HeLa cells were evenly divided into a control group, an NPs group, and an aqueous solvent group. After administration, the cells were cultured in a cell culture incubator for 24 h. The old medium was discarded and the cells were rinsed twice with PBS. The reactive oxygen species fluorescent probe was then added, followed by incubation for 30 min in an incubator. Following the removal, the staining solution was discarded and the cells were rinsed twice with PBS, and the anti-fluorescence quencher containing DAPI was added. The concentration of the staining solution was 1 ∶ 2 000. After processing the cells, cell staining was observed under a laser confocal microscope.

Statistical methods The experimental data are represented as mean ± *SD*, and all data were analyzed using SPSS 20.0 statistical software. *T*-tests and one-way ANOVA were used for analysis. $P<0.05$ was considered statistically significant ($^{*}P<0.05$, $^{**}P<0.01$, $^{***}P<0.001$). Origin 2018 software was used to plot the data.

Results

HC-NPs characterization

HC-NPs were characterized by TEM. The diameter was about 100 nm, as shown in Fig. 1. HC was encapsulated by DESP-PEG2000, forming oil-in-water microspheres. The results indicated that the preparation of HC-NPs was successful.

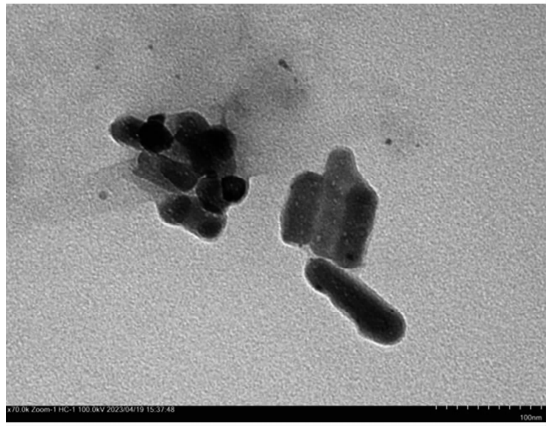

Fig. 1 Image of HC-NPs characterized by TEM

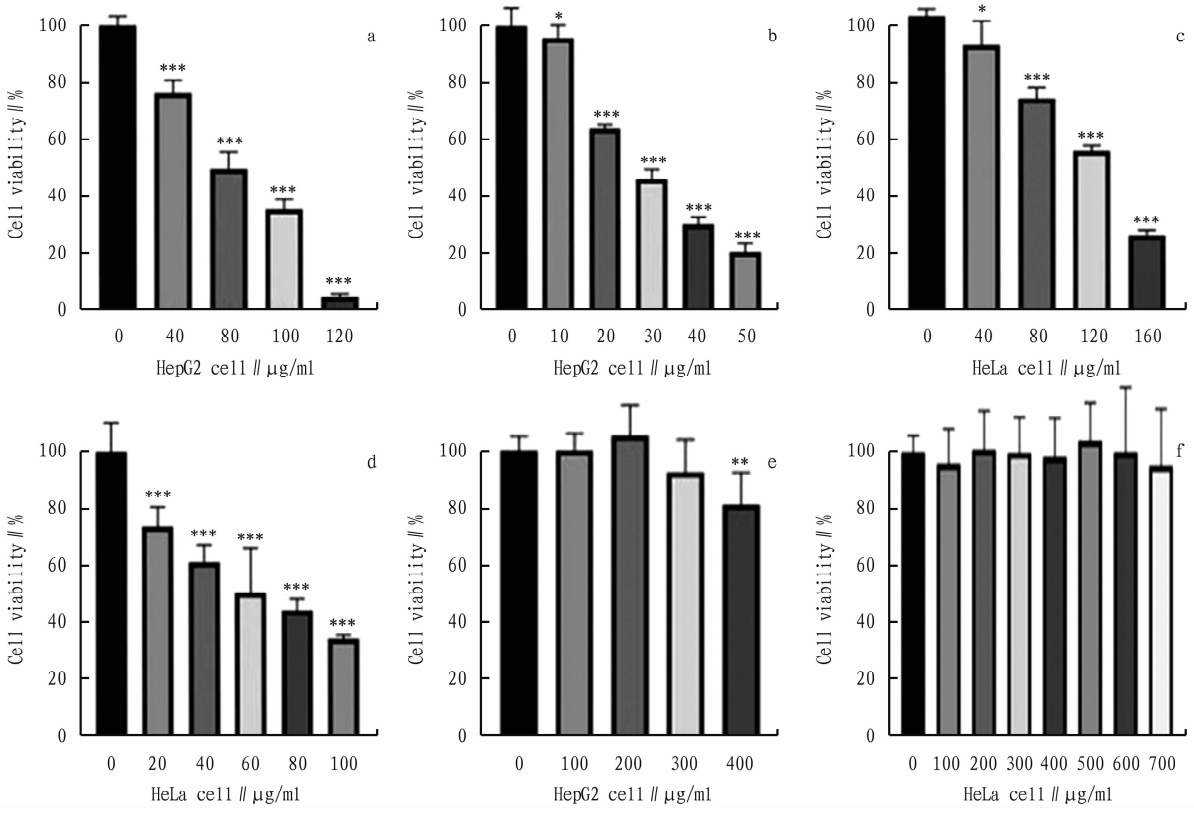

a. HC effects on HepG2 cell activity; b. HC-NPs effects on HepG2 cell activity; c. HC effects on HeLa cell activity; d. HC-NPs effects on HeLa cell activity; e. DESP-PEG2000 effects on HepG2 cell activity; f. DESP-PEG2000 effects on HeLa cell activity. Data are presented as mean ± SD ($n=4$). $^{*}P<0.05$, $^{**}P<0.01$, $^{***}P<0.001$ vs. control group.

Fig. 2 Cell proliferation inhibition histogram

Detection of cells proliferation and cytotoxicity

The effects of HC, HC-NPs, and blank solvents on HepG2 cells and HeLa cells were detailed in the findings presented in Fig. 2 (Fig. 2a and 2b for aqueous solvents, Fig. 2c and 2d for nano agents, and Fig. 2e and 2f for blank control groups). Following a 24 h treatment period, a notable decrease in cell viability was observed in the drug group compared with the control group, with the nano agents exhibiting a substantially lower IC_{50} than the aqueous solvent. Specifically, the IC_{50} of the aqueous solvent for HepG2 cells was 71.00 μg/ml, while that of the nanoagent was 27.48 μg/ml. Similarly, for HeLa cells, the IC_{50} of the aqueous solvent was 124.35 μg/ml, whereas that of the nanoagent was 61.00 μg/ml. These results demonstrate statistical significance, with the nanoagent displaying a stronger efficacy than the aqueous solvent, as evidenced by the IC_{50} values. Moreover, the blank experimental outcomes reveal that DESP-PEG2000 dissolved with THF exhibited non-toxicity towards HeLa cells and HepG2 cells within the experimental concentration range of the drug.

Cell migration situation detected by scratch assay

The results of tumor cell migration are shown in Fig. 3 and Fig. 4. HC treatments inhibited the migration efficiency of both types of tumor cells, but there was no significant difference ($P > 0.05$). Comparing different HC-treated cell groups, the migration ability of cells in the treatment group was much lower than that in the control group, and there were significantly more dead cells in the control group. Compared with the HC group, the migration ability of the HC-NPs group was much lower than that of the HC group.

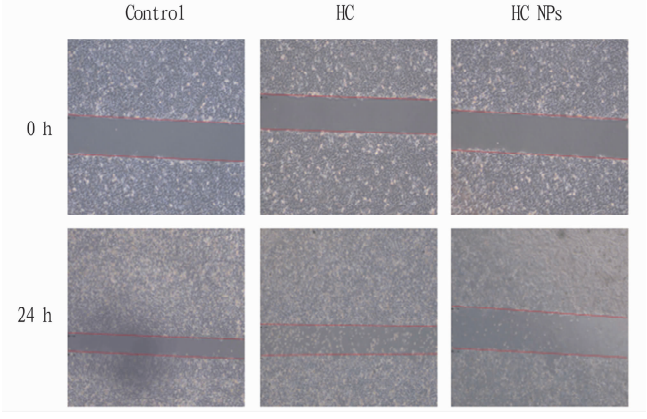

Fig. 3 Cell scratch assay to detect the effects of water solvent and nano agent on the migration rate of HepG2 cells in canary fruit

Detection of cytotoxicity using live/dead cell co-staining assay

After confirming the inhibitory effect of HC on the proliferation of HepG2 and HeLa cells in the early stage, live/dead cell co-staining experiments were carried out to identify live and dead cells, and further verify the cytotoxicity of the drug. The control group expressed a large area of strong green fluorescence and weak red fluorescence, and the results showed that the cells were mostly living cells. In the experimental group, a large number of cells were stained and emitted red fluorescence. Compared with the HC IC_{50} concentration group, the HC-NPs IC_{50} group showed significant apoptosis results and a significant decrease in cell numbers (Fig. 5 – Fig. 6).

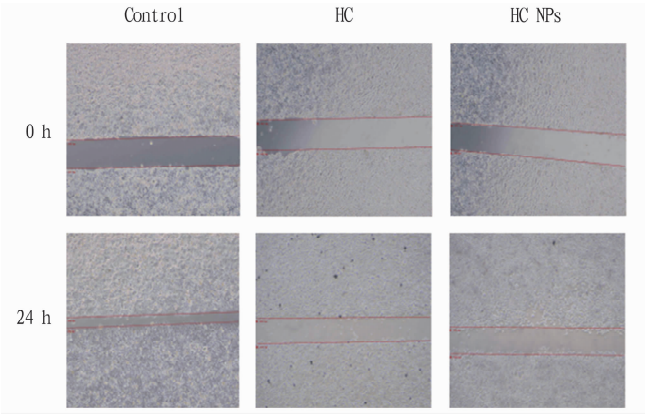

Fig. 4 Cell scratch assay to detect the effects of water solvent and nano agent on HeLa cell migration rate in canary fruit

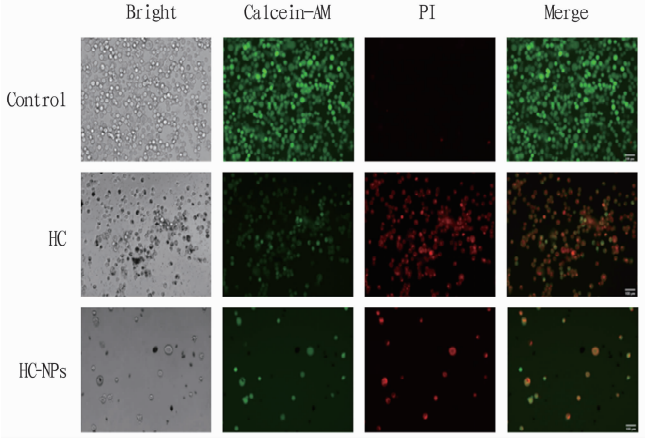

Fig. 5 *In-vitro* Calcein AM/PI co-staining experiment to detect the cytotoxicity of canary water solvent and nano agent on HepG2 cells

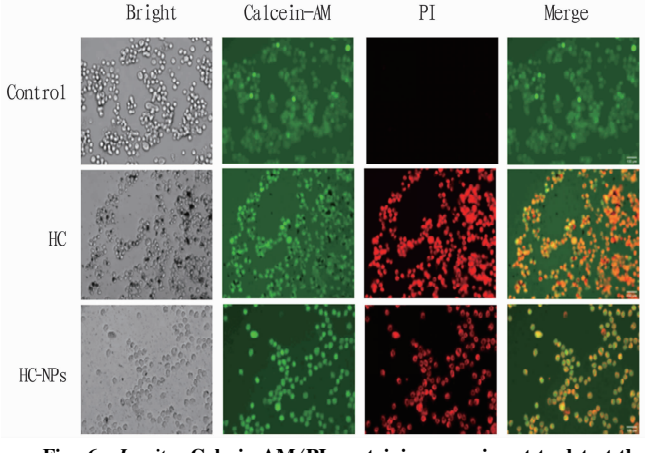

Fig. 6 *In-vitro* Calcein AM/PI co-staining experiment to detect the cytotoxicity of canary water solvent and nano agent on HeLa cells

Drug localization experiment

The results of drug localization experiments demonstrated that

hypericin successfully entered cells and specifically bound to lysosomes (Fig. 7 – Fig. 8).

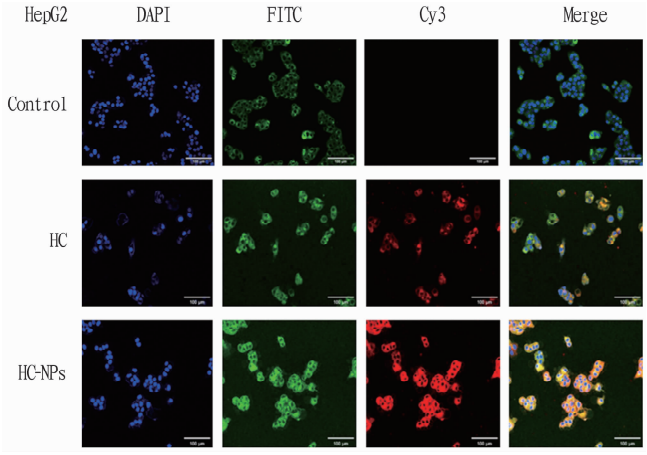

Fig. 7 The results of lysosomal localization of drugs in HepG2

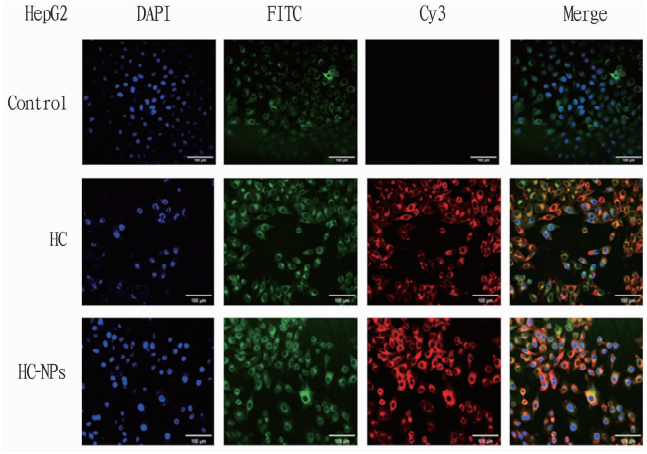

Fig. 8 The results of lysosomal localization of drugs in HeLa

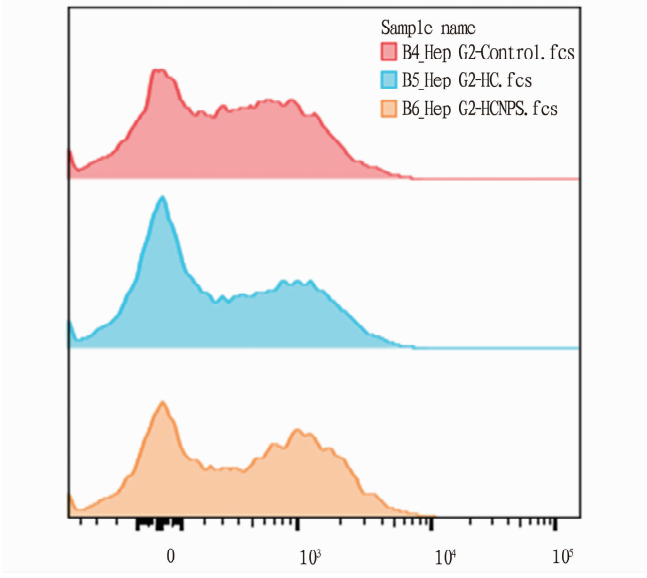

Fig. 9 Results of ROS produced by drugs in HepG2 cells under dark light without antioxidant

Flow cytometry was used to detect the content of ROS after administration

The results showed that the drug did not produce reactive oxygen species in HepG2 cells with or without the addition of antioxidants (Fig. 9 – Fig. 10), but it did generate reactive oxygen species in HeLa cells under dark conditions upon antioxidant addition, and these species vanished following antioxidant addition. (Fig. 11 – Fig. 12).

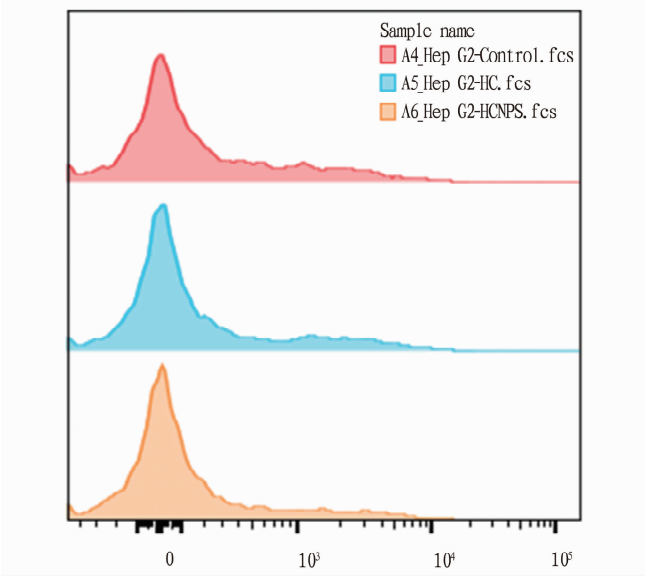

Fig. 10 Results of ROS produced by drugs in HepG2 cells under dark light with the addition of antioxidants

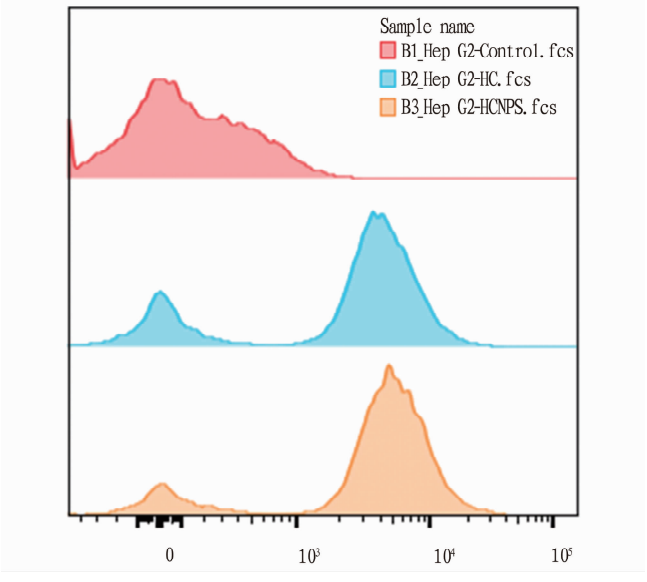

Fig. 11 Results of ROS produced by drugs in HeLa cells under dark light without antioxidant

Confocal laser scanning microscopy was used to detect the content of ROS after administration

The results demonstrated that under dim light conditions, the drug did not emit green fluorescence as observed under confocal microscopy (Fig. 13 – Fig. 14), and it did not generate a considerable

amount of reactive oxygen species in HepG2 cells and HeLa cells under such conditions.

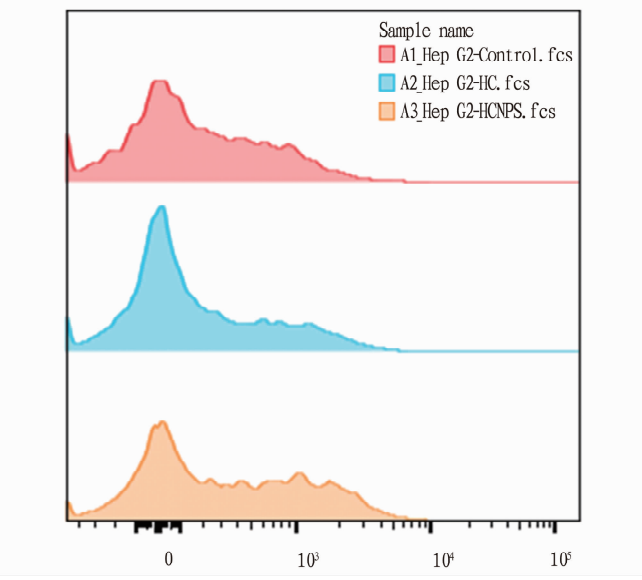

Fig. 12 Results of ROS produced by drugs in HeLa cells under dark light with the addition of antioxidants

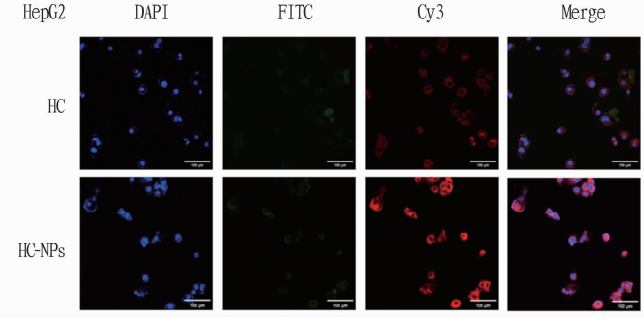

Fig. 13 Confocal microscopy was used to capture the ROS generation in HepG2 cells under dim light after drug treatment

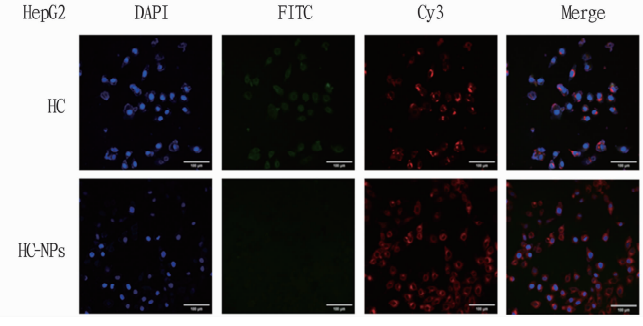

Fig. 14 Confocal microscopy was used to capture the ROS generation in HeLa cells under dim light after drug treatment

Discussion

In the context of the ongoing battle against liver and cervical cancer, the use of hypericin (HC), an extract derived from Chinese herbal medicine, has shown promise in this study. HC is recognized for its anti-cancer properties, particularly due to its ability to induce apoptosis in a variety of tumor cells, marking it as a potent agent in the fight against cancer[18]. The mechanism by which HC exerts its effects is through its specific binding function in poorly differentiated tumor cells. It exhibits a high affinity for these cells and tends to accumulate preferentially in tumor tissues. The excretion of HC by cancer cells is significantly lower than normal tissues, which results in the selective accumulation of HC within cancer cells, leading to the induction of cell necrosis, apoptosis, and autophagy[19].

The anticipated outcome of this experiment is that HC will inhibit the growth and migration of HepG2 liver cancer cells and HeLa cervical cancer cells and promote apoptosis. The binding sites of hypericin drugs to cells were also determined. It was expected that the nanoformulation of HC would demonstrate a more pronounced effect than the aqueous solvents. It was expected that the nanoformulation of HC would demonstrate a more pronounced effect than the aqueous solvents. These expectations were confirmed through a series of experiments, including the CCK-8 assay, cell scratch assays, Calcein AM/PI live/dead cell co-staining experiments, and flow cytometry experiments. These results provide a theoretical foundation for further *in-vitro* studies.

Given the water insolubility of HC, the research team employed nano-precipitation technology to enhance its solubility and create a more uniform and smaller-sized solution formulation. This approach aimed to maximize drug delivery to the target site and improve the water solubility of HC[20]. However, observations from electron microscopy indicated that the drug particle size could still be reduced. The research group plans to continue refining the nano-formulation to achieve smaller and more uniform particles.

While photodynamic therapy has shown significant success in treating certain malignant tumors, and HC is a strong natural photosensitizer, the current experimental phase is focused on understanding the effect of HC on cell proliferation and apoptosis inhibition. The study utilized HepG2 and HeLa cells, and future studies will aim to include normal liver and cervical cells, as well as other liver cancer cell lines, to provide a more comprehensive understanding of HC's therapeutic effects.

In the study, it was found that hypericin could produce ROS in HeLa cells detected by flow cytometry under dark light condition, but no fluorescence was produced under laser confocal microscope. Therefore, it was speculated that the ROS signal was diffuse and low intensity, and no obvious fluorescence aggregation was formed. Meanwhile, compared with HepG2 cells, HeLa cells produced ROS probably because HeLa cells had higher drug uptake rate, higher mitochondrial sensitivity, and weak antioxidant capacity. Therefore, in order to reduce the stress response of cells, antioxidants were added, and ROS disappeared.

The study has preliminarily verified the therapeutic effect of HC on liver and cervical cancer cells. HC-NPs have been shown to inhibit gene expression in cancer cells[21] and induce apoptosis, necrosis, or autophagy[22]. However, the full spectrum of anti-cancer

(Continued on page 16)

approaches, two-dimensional electrophoresis and shotgun analysis[J]. Journal of Proteomics, 2018, 185: 51 – 63.
[30] YANG Z, ZHANG YW, ZHU J, *et al.* Effects of exogenous glutathione and precursor spraying on *Solanum nigrum* L. for remediation of heavy metal contaminated soil[J]. Environmental Science, 2025(4): 1 – 17. (in Chinese).
[31] JACQUART A, BRAYNER R, EL HAGE CHAHINE JM, *et al.* Cd^{2+} and Pb^{2+} complexation by glutathione and the phytochelatins [J]. Chemico-Biological Interactions, 2017, 267: 2 – 10.
[32] ZHENG G, ZHANG J, LIU Y, *et al.* Significance of glutathione in the hormesis effect: A case study of the relationship between heavy metal Cd and monitoring plant *Tillandsia ionantha*[J]. Plant Physiology and Biochemistry, 2025, 227: 110130.
[33] HAN YY, FAN TT, ZHU XY, *et al.* WRKY12 represses GSH1 expression to negatively regulate cadmium tolerance in *Arabidopsis*[J]. Plant Molecular Biology, 2019, 99(1 – 2): 149 – 159.
[34] HUANG KT, CHEN YX, HUANG L, *et al.* Effects of combined aluminum and manganese stress on osmoregulatory substances in sunflower seedling leaves [J]. Anhui Agricultural Science Bulletin, 2020, 26(17): 16 – 18. (in Chinese).
[35] SÁNCHEZ-THOMAS R, HERNÁNDEZ-GARNICA M, GRANADOS-RIVAS JC, *et al.* Intertwining of cellular osmotic stress handling mechanisms and heavy metal accumulation [J]. Molecular Biotechnology, 2024: 17.
[36] XU YN, MENG X, WANG YM, *et al.* Effects of exogenous proline on photosynthetic characteristics and protective enzyme system of wheat seedlings under drought stress[J]. Anhui Agricultural Science Bulletin, 2025, 31(14): 20 – 23. (in Chinese).
[37] GUO Q, LIU Y, SUN N, *et al.* The role of proline in plant resistances to oxidative stress induced by abiotic stresses[J]. Journal of Plant Genetic Resources, 2025, 26(11): 2085 – 2095. (in Chinese).
[38] XU J. Study on cadmium stress response mechanism of *Bidens pilosa* L. based on integrated analysis of transcriptomics and proteomics [D]. Nanning: Guangxi Normal University, 2022. (in Chinese).

Editor: Yingzhi GUANG Proofreader: Xinxiu ZHU

(Continued from page 7)

mechanisms of HC is not yet fully understood. The research group is committed to continuing investigations to explore the effects of HC-NPs on a broader range of cancers and to uncover the underlying mechanisms of its anti-cancer activity.

References

[1] ANWANWAN D, SINGH SK, SINGH S, *et al.* Challenges in liver cancer and possible treatment approaches[J]. Biochim Biophys Acta Rev Cancer, 2020, 1873(1): 188314.
[2] WU M. Clinical advances in primary liver cancer in China[J]. Hepatogastroenterology, 2001, 48(37): 29 – 32.
[3] YANG H, CHENG J, ZHUANG H, *et al.* Pharmacogenomic profiling of intra-tumor heterogeneity using a large organoid biobank of liver cancer [J]. Cancer Cell, 2024, 42(4): 535 – 551. e8.
[4] XIA P, ZHOU J, SHEN R, *et al.* Deciphering the cellular and molecular landscape of cervical cancer progression through single-cell and spatial transcriptomics[J]. NPJ Precis Oncol, 2025, 9(1): 158.
[5] WANG Z, LU J, HUANG L. Diagnosis and treatment of hepatocellular carcinoma with pelvic metastasis expressing AFP: A case report[J]. Frontiers in Oncology, 2025, 14(14): 1489725.
[6] FERRARA R, IMBIMBO M, MALOUF R, *et al.* Single or combined immune checkpoint inhibitors compared to first-line platinum-based chemotherapy with or without bevacizumab for people with advanced non-small cell lung cancer [J]. Cochrane Database Syst Rev, 2021, 4 (4): CD013257.
[7] ZHANG J. Current status and issues in the treatment of cervical cancer: From clinical guidelines to real-world research[J]. General Practice in China, 2022, 25(3): 259 – 263.
[8] ZHOU F, TENG F, DENG P, *et al.* Recent progress of nano-drug delivery system for liver cancer treatment[J]. Anticancer Agents Med Chem, 2018, 17(14): 1884 – 1897.
[9] WU JJ, ZHANG J, XIA CY, *et al.* Hypericin: A natural anthraquinone as promising therapeutic agent[J]. Phytomedicine, 2023, 111: 154654.
[10] AGOSTINIS P, VANTIEGHEM A, MERLEVEDE W, *et al.* Hypericin in cancer treatment: More light on the way[J]. Int J Biochem Cell Biol, 2002, 34(3): 221 – 241.
[11] YOUSSEF T, FADEL M, FAHMY R, *et al.* Evaluation of hypericin-loaded solid lipid nanoparticles: Physicochemical properties, photostability and phototoxicity[J]. Pharm Dev Technol, 2012, 17(2): 177 – 186.
[12] KHALIL HMA, MAHMOUD DB, EL-SHIEKH RA, *et al.* Antidepressant and cardioprotective effects of self-nanoemulsifying self-nanosuspension loaded with Hypericum perforatum on post-myocardial infarction depression in rats[J]. AAPS PharmSciTech, 2022, 23(7): 243.
[13] NAJAHI-MISSAOUI W, ARNOLD RD, CUMMINGS BS. Safe Nanoparticles: Are we there yet? [J]. Int J Mol Sci, 2020, 22(1): 385.
[14] ATUKORALE PU, COVARRUBIAS G, BAUER L, *et al.* Vascular targeting of nanoparticles for molecular imaging of diseased endothelium [J]. Adv Drug Deliv Rev, 2017, 113: 141 – 156.
[15] LI B, WANG F, GUI L, *et al.* The potential of biomimetic nanoparticles for tumor-targeted drug delivery[J]. Nanomedicine (Lond), 2018, 13(16): 2099 – 2118.
[16] SABOURIAN P, YAZDANI G, ASHRAF SS, *et al.* Effect of physicochemical properties of nanoparticles on their intracellular uptake[J]. Int J Mol Sci, 2020, 21(21): 8019.
[17] ZHU L, LIN M. The Synthesis of nano-doxorubicin and its anticancer effect[J]. Anticancer Agents Med Chem, 2021, 21(18): 2466 – 2477.
[18] CHOUDHARY N, COLLIGNON TE, TEWARI D, *et al.* Hypericin and its anticancer effects: From mechanism of action to potential therapeutic application[J]. Phytomedicine, 2022, 105: 154356.
[19] MAO SC. The structure and photoactivity of hypericin were studied by density functional theory[J]. Journal of Zhongkai Agricultural Engineering College, 2011, 24(2): 13 – 16.
[20] KANG W, TIAN Y, ZHAO Y, *et al.* Applications of nanocomposites based on zeolitic imidazolate framework-8 in photodynamic and synergistic anti-tumor therapy[J]. RSC Adv, 2022, 12(26): 16927 – 16941.
[21] MATIĆ IZ, ERGÜN S, Đ OR Đ I ĆCRNOGORAC M, *et al.* Cytotoxic activities of *Hypericum perforatum* L. extracts against 2D and 3D cancer cell models[J]. Cytotechnology, 2021, 73(3): 373 – 389.
[22] JENDŽELOVSKÁ Z, JENDŽELOVSKÝ R, KUCHÁROVÁ B, *et al.* Hypericin in the light and in the dark: Two sides of the same coin[J]. Front Plant Sci, 2016, 7: 560.

Editor: Yingzhi GUANG Proofreader: Xinxiu ZHU